KEK-CP-303, NIKHEF 14-005

TTP14-004, SFB/CPP-14-06

# Full $\mathcal{O}(\alpha)$ electroweak radiative corrections to $e^+e^- \to e^+e^-\gamma$ at the ILC with GRACE-Loop

P.H. Khiem[A,B], Y. Kurihara[A], J. Fujimoto[A], T. Ishikawa[A],

T. Kaneko[A], K. Kato[C], N. Nakazawa[C], Y. Shimizu[A],

T. Ueda[D], J.A.M. Vermaseren[E], Y. Yasui[F]

[A)] *KEK, Oho 1-1, Tsukuba, Ibaraki 305-0801, Japan.*

[B)] *SOKENDAI University, Shonan Village, Hayama, Kanagawa 240-0193 Japan.*

[C)] *Kogakuin University, Shinjuku, Tokyo 163-8677, Japan.*

[D)] *Karlsruhe Institute of Technology (KIT), D-76128 Karlsruhe, Germany.*

[E)] *Nikhef, Science Park 105, 1098 XG Amsterdam, The Netherlands.*

[F)] *Tokyo Management College, Ichikawa, Chiba 272-0001, Japan.*

arXiv:1403.6557v3 [hep-ph] 3 Apr 2014

**Abstract**

We present a calculation of the full $\mathcal{O}(\alpha)$ electroweak radiative corrections to the process $e^+e^- \to e^+e^-\gamma$ at the International Linear Collider (ILC). The computation is performed with the help of the GRACE-Loop system. In this system, the calculations are checked numerically by three kinds of consistency tests: ultraviolet finiteness, infrared finiteness, and gauge parameter independence. The results show good numerical stability when quadruple precision is used. We find that the electroweak corrections range from $-2\%$ to $\sim -20\%$ when varying $\sqrt{s}$ from 250 GeV to 1 TeV. Such corrections will play an important role for the high precision program at the ILC.

# 1 Introduction

The main goals of future colliders, such as the ILC, are not only to make precise measurements of the properties of the Higgs particle, top quarks and vector bosons interactions, but also to search for physics Beyond the Standard Model (BSM). The measurements will be performed to high precision with the statistical error typically below 0.1% at the ILC. This will require a very precise measurement of the luminosity. At the ILC, the integrated luminosity is measured by counting Bhabha events and comparing it with the corresponding theoretical cross-section. Thus a precise calculation of Bhabha scattering is mandatory.

The full one-loop electroweak corrections to the $e^+e^- \to e^+e^-$ reaction were calculated by K. Tobimatsu et al in Ref [1, 2] and M. Bohm et al in Ref [3, 4] a long time ago. These calculations were independently calculated by F.A. Berends et al in Ref [5], and Fleischer et al in Ref [6].

The cases of one-loop electroweak corrections to Bhabha scattering are understood well from theoretical calculations. The corrections as we have known form a massive contribution to total cross-section, about $\mathcal{O}(10\%)$ at high energy. It is undoubted that the two-loop electroweak corrections to Bhabha scattering must be taken into consideration. Such calculations are also great concerned by many authors. However, almost the calculations have only perfromed at two-loop QED corrections. A full two-loop electroweak corrections are by far in considering and developing. We introduce some typical papers for two-loop QED calculations in this section. A two-loop photonic corrections to this process were completed by A.A. Penin in Refs [7, 8]. The two-loop QED corrections which keeping electron mass in the square amplitude were done by R. Bonciani et al in Ref [9]. In a later publication, they included the soft photon emission's contribution to differential cross-section, as presented in Ref [10]. The two-loop QED corrections to Bhabha cross-section which involve the vacuum polarization by heavy fermions of arbitrary mass were

also considered and presented in Refs [11, 12]. Moreover, an approximation calculation of two-loop electroweak corrections to Bhabha scattering is computed in Ref [14]. In this calculation, the authors considered the dominant logarithmically enhanced two-loop electroweak corrections to the differential cross section in the high energy limit with large scattering angles.

Beside a precise calculation of the Bhabha scattering cross-section, the evaluation of backgrounds to the Bhabha events is also important for the luminosity measurement at the ILC. Experiment can make a misidentification $e^+e^-\gamma$ as $e^+e^-$ events for following reasons: the photon is hard photon and it can escape from the detector; the photon is soft photon with opening angle to the final electron (or positron) is small; or the photon go parallel to the beamline. With this misidentification the process $e^+e^- \to e^+e^-\gamma$ is one of the channels that form a massive contribution to the background for Bhabha events. In order to correct the number of counted Bhabha events, theoretical calculation to the process have to be concerned. The lowest-order calculation of this process was obtained in Ref [15]. The one-loop QED corrections to the hard-bremsstrahlung process $e^+e^- \to e^+e^-\gamma$ were found in Ref [13]. A analytical calculation of one-loop QED corrections to the process $e^+e^- \to e^+e^-\gamma$ is also considered in Ref [16].

In this paper, we present the calculation of the full $\mathcal{O}(\alpha)$ electroweak radiative corrections to this process. The computation is performed with the help of the GRACE-Loop system. We then discuss the electroweak corrections to the total cross-section which are shown as a function of the center-of-mass energy, $(\sqrt{s})$. The distributions of the invariant masses, energy of final particles are also discussed in this paper.

The paper is organized as follows. In section 2, we present a short introduction to the GRACE-Loop system and the numerical tests of the results. In section 3 we present the physics results of the calculation. Conclusions and future plans will be addressed in section 4.

# 2 GRACE-Loop and the process $e^+e^- \to e^+e^-\gamma$

## 2.1 GRACE-Loop

GRACE-Loop is a generic program for the automatic calculation of high energy physics processes at the one-loop level. The program is described in detail in Ref [17] where a variety of $2 \to 2$-body electroweak processes are presented and compared with other papers. The GRACE-Loop system has also been used to calculate $2 \to 3$-body processes such as $e^+e^- \to ZHH$ [18], $e^+e^- \to t\bar{t}H$ [19], $e^+e^- \to \nu\bar{\nu}H$ [20]. The above calculations have been done independently by other groups, for example the processes $e^+e^- \to ZHH$ [21], $e^+e^- \to t\bar{t}H$ [22, 23, 24] and $e^+e^- \to \nu\bar{\nu}H$ [25, 26]. Also the $2 \to 4$-body process $e^+e^- \to \nu_\mu\bar{\nu}_\mu HH$ [27] was calculated successfully with the use of the GRACE-loop system.

In the GRACE-Loop system the renormalization is carried out with the on-shell renormalization condition of the Kyoto scheme as described in Ref [28]. The ultraviolet (UV) divergences are regulated by dimensional regularization. While the infrared (IR) divergences are regularized by giving the photon an infinitesimal mass $\lambda$.

Ref [17] describes the method used in the GRACE-Loop system to reduce the tensor one-loop five- and six-point functions into one-loop four-point functions. The tensor one-, two-, three- and four-point functions are then reduced to scalar one-loop integrals which will be numerically evaluated by one of the FF [29] or LoopTools [30] packages.

The program has been equipped with so-called non-linear gauge fixing terms [31] in the Lagrangian which are defined as

$$\begin{aligned}\mathcal{L}_{GF} &= -\frac{1}{\xi_W}|(\partial_\mu - ie\tilde{\alpha}A_\mu - igc_W\tilde{\beta}Z_\mu)W^{\mu+} + \xi_W\frac{g}{2}(v+\tilde{\delta}H+i\tilde{\kappa}\chi_3)\chi^+|^2 \\ &\quad -\frac{1}{2\xi_Z}(\partial\cdot Z + \xi_Z\frac{g}{2c_W}(v+\tilde{\varepsilon}H)\chi_3)^2 - \frac{1}{2\xi_A}(\partial\cdot A)^2 \,. \end{aligned} \tag{1}$$

We are working in the $R_\xi$-type gauges with the condition $\xi_W = \xi_Z = \xi_A = 1$ (also

called the 't Hooft-Feynman gauge), There is no longitudinal contribution in the gauge propagator. This choice has not only the advantage of making the expressions much simpler. It also avoids unnecessary large cancellations, high tensor ranks in the one-loop integrals and extra powers of momenta in the denominators which cannot be handled by the FF package. With the implementation of non-linear gauge fixing terms the system provides a powerful tool to check the results in a consistent way. After all, the results must be independent of the non-linear gauge parameters. This will be discussed in greater detail in the section on the numerical checks of the calculation.

In its latest version GRACE-Loop can use the axial gauge in the projection operator of external photons. It cures a problem with large numerical cancellations. This is very useful when calculating processes at small angles and energy cuts for the final state particles. It also provides a useful tool to check the consistency of the results which, due to the Ward identities, must be independent of the choice of the gauge. This method has been applied successfully to the process $e^+e^- \to t\bar{t}\gamma$ in Ref [32]. We also applied the method in the current calculation.

In the integration step we use a parallel version of BASES [33] with MPI [34] (Message Passing Interface) to reduce the calculation time.

## 2.2 The process $e^+e^- \to e^+e^-\gamma$

The full set of Feynman diagrams with the non-linear gauge fixing as described in the previous section consists of 32 tree diagrams and 3456 one-loop diagrams including the counterterm diagrams. In Fig 1 we show some selected diagrams.

The calculation is checked numerically by three kinds of consistency tests. These are ultraviolet and infrared finiteness, and independence of the gauge parameters. In general the total cross-section with the full one-loop electroweak radiative corrections is written

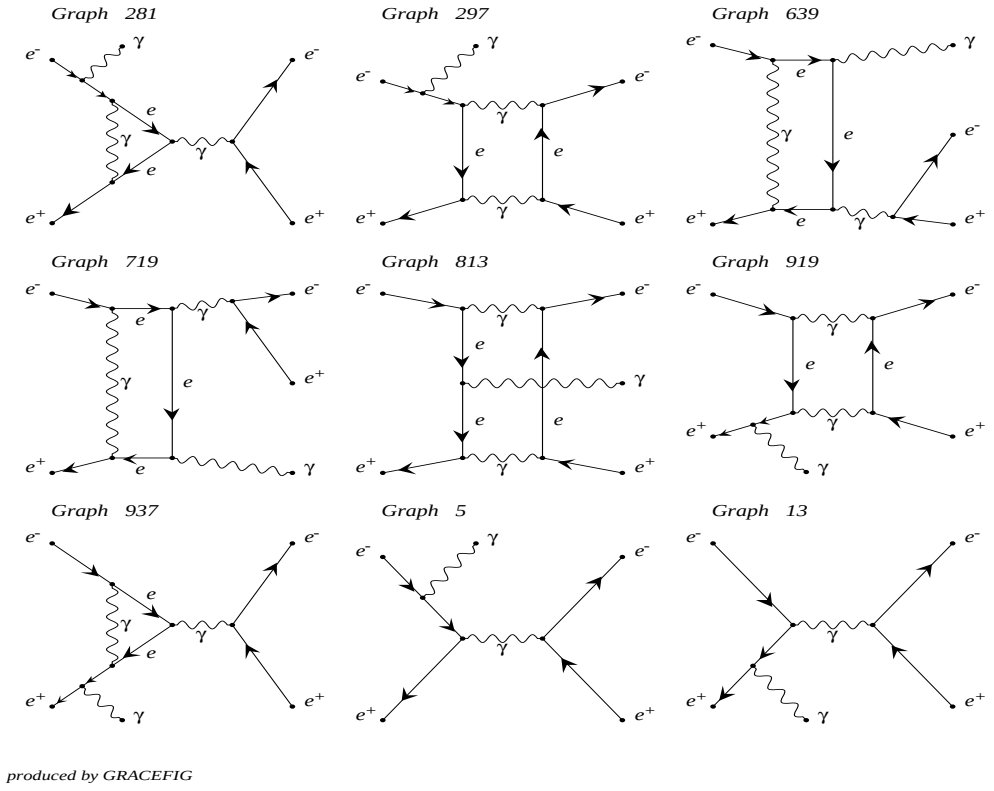


Figure 1: Typical Feynman diagrams as generated by the GRACE-Loop system.

by

$$\begin{aligned}\sigma_{\mathbf{tot}}^{e^-e^+\gamma_H} &= \int d\sigma_{\mathbf{T}}^{e^-e^+\gamma_H} + \int d\sigma_{\mathbf{V}}^{e^-e^+\gamma_H}(C_{UV}, \{\tilde{\alpha}, \tilde{\beta}, \tilde{\delta}, \tilde{\epsilon}, \tilde{\kappa}\}, \lambda) \\ &\quad + \int d\sigma_{\mathbf{T}}^{e^-e^+\gamma_H}\delta_{\mathbf{soft}}(\lambda \leq E_{\gamma_S} < k_c) + \int d\sigma_{\mathbf{H}}^{e^-e^+\gamma_H\gamma_S}(E_{\gamma_S} \geq k_c). \end{aligned} \tag{2}$$

In this formula $\sigma_{\mathbf{T}}^{e^-e^+\gamma_H}$ is the tree-level cross-section. $\sigma_{\mathbf{V}}^{e^-e^+\gamma_H}$ is the cross-section due to the interference of the one-loop (including counterterms) and the tree diagrams. The contribution must be independent of the ultraviolet cutoff parameter ($C_{UV}$) and the non-linear gauge parameters ($\tilde{\alpha}, \tilde{\beta}, \tilde{\delta}, \tilde{\epsilon}, \tilde{\kappa}$). Because of the way we regularize the IR-divergences

$\sigma_{\mathbf{V}}^{e^-e^+\gamma_H}$ depends on the photon mass $\lambda$. The $\lambda$ dependence of the result has to cancel against the soft photon contribution, the third term in Eq.2. The soft contribution can be factorised into a soft factor, which is written by the formula below, and the crosssection from the tree diagrams.

$$\delta_{\mathbf{soft}}(\lambda \leq E_{\gamma_S} < k_c) \;=\; -e^2 \int_{\lambda \leq q_0 \leq k_c} \frac{d^3q}{(2\pi)^3 2q^0} \left| \frac{p^-}{q \cdot p^-} - \frac{p^+}{q \cdot p^+} \right|^2 , \tag{3}$$

where $q$ and $p^\pm$ are the photon and the $e^\pm$ 4-momenta respectively.

In the tables (1, 2, 3), we present the numerical results of the ultraviolet finiteness checks, the gauge invariance and the infrared finiteness at one random phase space point. This test is performed in quadruple precision. We find that the results are stable over a range of 19 digits. The different precisions are due to the ways these parameters occur in the formulas. $C_{UV}$ occurs only linearly as an extra term, The non-linear gauge parameters occur as products in terms that are by themselves typically much larger than the remaining terms. The infrared regulator $\lambda$ will mainly contribute due to its appearance in the denominators. As a result the $C_{UV}$ checks give a much better accuracy than the other checks.

| $C_{UV}$ | $2\Re(\mathcal{M}_{Loop}\mathcal{M}^+_{Tree})$ |
|---|---|
| 0 | $-1.880016140700886331600963802525 06$ |
| $10^2$ | $-1.880016140700886331600963802525 04$ |
| $10^4$ | $-1.880016140700886331600963802524 83$ |

Table 1: Test of the $C_{UV}$ independence of the amplitude. In this table, we take the non-linear gauge parameters to be 0, $\lambda = 10^{-17}$GeV and we use 1 TeV for the center-of-mass energy.

Finally, we consider the contribution of the hard photon bremsstrahlung, $\sigma_{\mathbf{H}}^{e^-e^+\gamma\gamma}(k_c)$. This part is the process $e^+e^- \to e^-e^+\gamma\gamma$ and is generated by the tree level version of

| $(\tilde{\alpha}, \tilde{\beta}, \tilde{\delta}, \tilde{\kappa}, \tilde{\epsilon})$ | $2\Re(\mathcal{M}_{Loop}\mathcal{M}^{+}_{Tree})$ |
|---|---|
| (0, 0, 0, 0, 0) | $-1.880016140700886331600963802525 06$ |
| (1.1,1.2,1.3,1.4,1.5) | $-1.880016140700886331600963802525 27$ |
| (11,12,13,14,15) | $-1.880016140700886331600963802604 99$ |

Table 2: Gauge invariance of the amplitude. In this table, we set $C_{UV} = 0$, the photon mass is $10^{-17}$GeV and a 1 TeV center-of-mass energy.

| $\lambda$ [GeV] | $2\Re(\mathcal{M}_{Loop}\mathcal{M}^{+}_{Tree})$+ soft contribution |
|---|---|
| $10^{-17}$ | $-0.392635564863145920331840202138979$ |
| $10^{-20}$ | $-0.392635564863145860698638985751228$ |
| $10^{-25}$ | $-0.392635564863145860639598148071754$ |

Table 3: Test of the IR finiteness of the amplitude. In this table we take the non-linear gauge parameters to be 0, $C_{UV} = 0$ and the center-of-mass energy is 1 TeV.

GRACE [35] with the use of the phase space integration by BASES. By adding this contribution to the total cross-section, the final results have to be independent of $k_c$. In table (4) the numerical result of the $k_c$ stability check is shown. By changing the value of $k_c$ from $10^{-3}$ GeV to 0.1 GeV, we find that the results are in agreement to an accuracy which is better than 0.05%. For the $k_c$ stability checks, it is important to note that we have two photons at the final state. One of them is the hard photon which will be applied an energy cut of $E_\gamma^{cut} \geq 10$ GeV and an angle cut of $10^\circ \leq \theta_\gamma^{cut} \leq 170^\circ$. The other one is a soft photon of which the energy is greater than $k_c$ and smaller than the first photon's energy.

The reduction method for the one-loop five point function in GRACE-Loop is also cross-checked with the one in Ref [36] by calculating the product of diagram 813 and diagrams 5 and 13 in figure (1). Table 5 shows the numerical check at an arbitrary phase

| $k_c$ [GeV] | $\sigma_S$ [pb] | $\sigma_H$ [pb] | $\sigma_{S+H}$ [pb] |
|---|---|---|---|
| $10^{-1}$ | 6.829 | 1.454 | 8.284 |
| $10^{-2}$ | 6.302 | 1.983 | 8.286 |
| $10^{-3}$ | 5.776 | 2.512 | 8.289 |

Table 4: Test of the $k_c$-stability of the result. We choose the photon mass to be $10^{-17}$ GeV and the center-of-mass energy is 1 TeV. The second column presents the hard photon cross-section and the third column presents the soft photon cross-section. The final column is the sum of both.

space point. The two methods are in agreement over a range of 19 digits.

| | $2\Re(\mathcal{M}_{Loop}\mathcal{M}^{+}_{Tree})$ |
|---|---|
| GRACE-Loop | $4.22739111621446897277673850297904 4\cdot 10^{-6}$ |
| Ref [36] | $4.22739111621446897227226635627123 0\cdot 10^{-6}$ |

Table 5: Test of the reduction of the one loop five point functions in GRACE-Loop in comparison with the method in Ref [36].

After checking the results successfully, we can proceed with the computations of the physics results of the process. Hereafter we set $\lambda = 10^{-17}$ GeV, $C_{UV} = 0$, $k_c = 10^{-3}$ GeV and $\tilde{\alpha} = \tilde{\beta} = \tilde{\delta} = \tilde{\kappa} = \tilde{\varepsilon} = 0$. In order to reduce the calculation time, we neglected the diagrams which contained the coupling of Higgs boson to electron and positron ($\lambda_{He^-e^+}$) in the integration step. Because it's contribution is smaller than the statistical error of Monte Carlo integration.

# 3 The physics results

Our input parameters for the calculation are as follows. The fine structure constant in the Thomson limit is $\alpha^{-1} = 137.0359895$. For the boson masses, we input $M_H = 126$ GeV, $M_Z = 91.1876$ GeV and $M_W = 80.385$ GeV. For the lepton masses we take $m_e = 0.510998928$ MeV, $m_\tau = 1776.82$ MeV and $m_\mu = 105.6583715$ MeV. For the quark masses we take $m_u = 2.3$ MeV, $m_d = 4.8$ MeV, $m_c = 1.275$ GeV, $m_s = 95$ MeV, $m_t = 173.5$ GeV and $m_b = 4.18$ GeV. The decay width of the Z boson is 2.3549 GeV which is calculated by using the tree version of GRACE [35] with the same input parameters. We consider all the decay channels of the Z boson within the Standard Model to generate this decay width. Then, we applied it to the propagators with Z boson exchange (it is important note that we did not apply it to the propagators which appear in one-loop integrals). It helps to avoid the singularity due to Z boson resonance.

For the final state particles we apply an energy cut of $E^{cut} \geq 10$ GeV and an angle cut of $10^\circ \leq \theta^{cut} \leq 170^\circ$ with respect to the beamline. In order to isolate the photon from the electron (or positron) we apply an opening angle cut between the photon and the $e^-(e^+)$ of $10^\circ$. Moreover, to distinguish $e^-e^+\gamma$ events from $\gamma\gamma$ events, we apply an angle cut between the final state electron and positron of $10^\circ$.

The full $\mathcal{O}(\alpha)$ electroweak cross-section $\sigma(\alpha)$ takes into account the tree graphs and the full one-loop virtual corrections as well as the soft and hard bremsstrahlung contributions. The relative correction is defined as

$$\delta_{EW} = \frac{\sigma(\alpha)}{\sigma_{Tree}} - 1. \tag{4}$$

In order to obtain the genuine weak corrections, we first calculate the pure QED corrections which are defined by

$$\delta_{QED} = \frac{\sigma^{QED}(\alpha) - \sigma_0^{QED}}{\sigma_{Tree}}. \tag{5}$$

Here $\sigma_0^{QED}$ is the cross-section of the tree-level QED diagrams and $\sigma^{QED}(\alpha)$ is the cross-section due to the interference of the QED one-loop (including counterterm) diagrams and the QED tree diagrams. This part can be calculated separately in the GRACE-Loop system.

After obtaining the QED corrections, we evaluate the genuine weak corrections in the $\alpha$ scheme. These corrections are defined by

$$\delta_W \;=\; \delta_{EW} - \delta_{QED}. \tag{6}$$

In fig 2, the cross-section and the electroweak corrections are shown as a function of $\sqrt{s}$. The center-of-mass energy ranges from 250 GeV (which is near the threshold of $M_H + M_Z$) to 1 TeV. In the left part of fig 2 the corrections make the cross-section decrease more and more with increasing center-of-mass energy. We find that the electroweak corrections are from $-2\%$ to $\sim -20\%$ when varying $\sqrt{s}$ from 250 GeV to 1 TeV. The right part of fig 2 clearly shows that QED provides the dominant contribution as compared to the weak corrections. It goes to $-14\%$ at $\sqrt{s} = 1$ TeV, while the weak corrections change from $\sim 2\%$ to $\sim 6\%$ when $\sqrt{s}$ changes from 250 GeV to 1 TeV. It is clear that the corrections are a sizable contribution to the total cross-section and cannot be ignored for the high precision program at the ILC.

In fig 3, the distribution of the cross-section as a function of the photon energy are presented for $\sqrt{s} = 250$ GeV and $\sqrt{s} = 1$ TeV. The dashed line is the result of the tree level calculation and the solid line is the result of including the full radiative corrections. On the whole the cross-section decreases with increasing photon energy. At $\sqrt{s} = 250$ GeV we observe two peaks at $E_\gamma = \frac{s - M_Z^2}{2\sqrt{s}}$ and $\frac{\sqrt{s}}{2}$. The first peak corresponds to the photon recoiling against an on-shell $Z$ boson, and the second has the photon recoil against a virtual photon that creates a small mass electron-positron pair. Due to the high energy the peaks overlap within our resolution at $\sqrt{s} = 1$ TeV. The distributions also clearly show

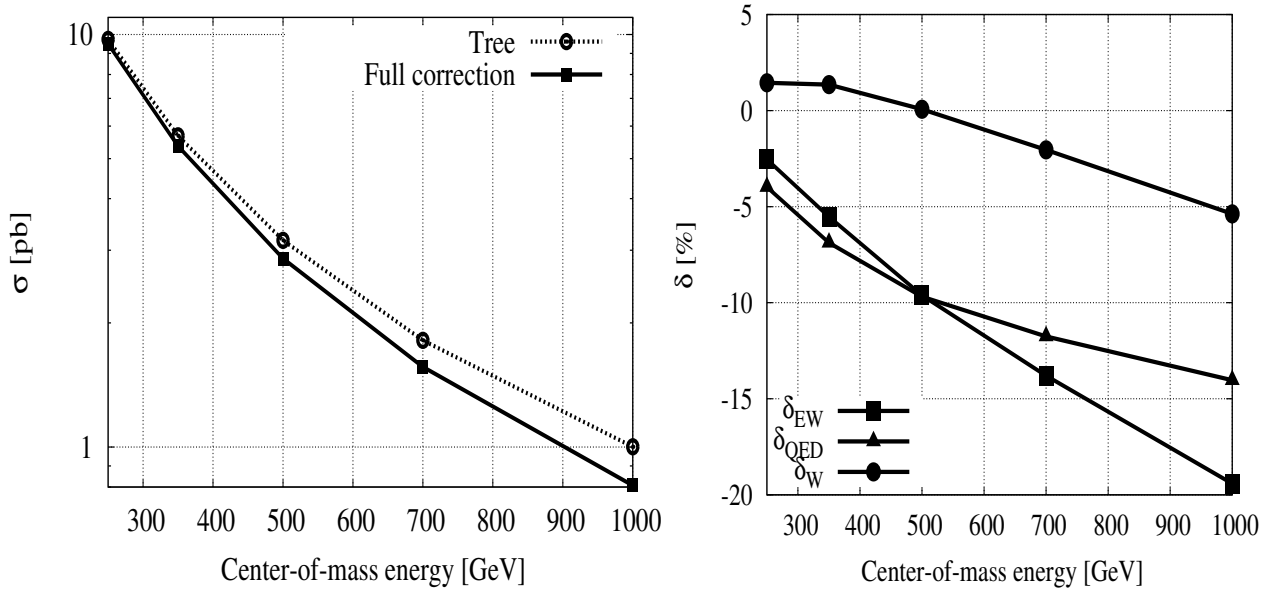


Figure 2: In this figure, the cross-section (left) and full electroweak corrections (right) are presented as a function of the center-of-mass energy.

that the radiative corrections are visible and are important for the luminosity monitor at the ILC.

In figure 4 the distributions of the invariant mass of the $e^-$, $e^+$ pair are shown at $\sqrt{s} = 250$ GeV and $\sqrt{s} = 1$ TeV. The dashed lines present the result of the tree-level calculations and the solid lines are the result of including the full radiative corrections. We find the peaks at the $M_Z$ pole and at the high mass region (corresponding to the radiative tail). Again the radiative corrections are clearly visible.

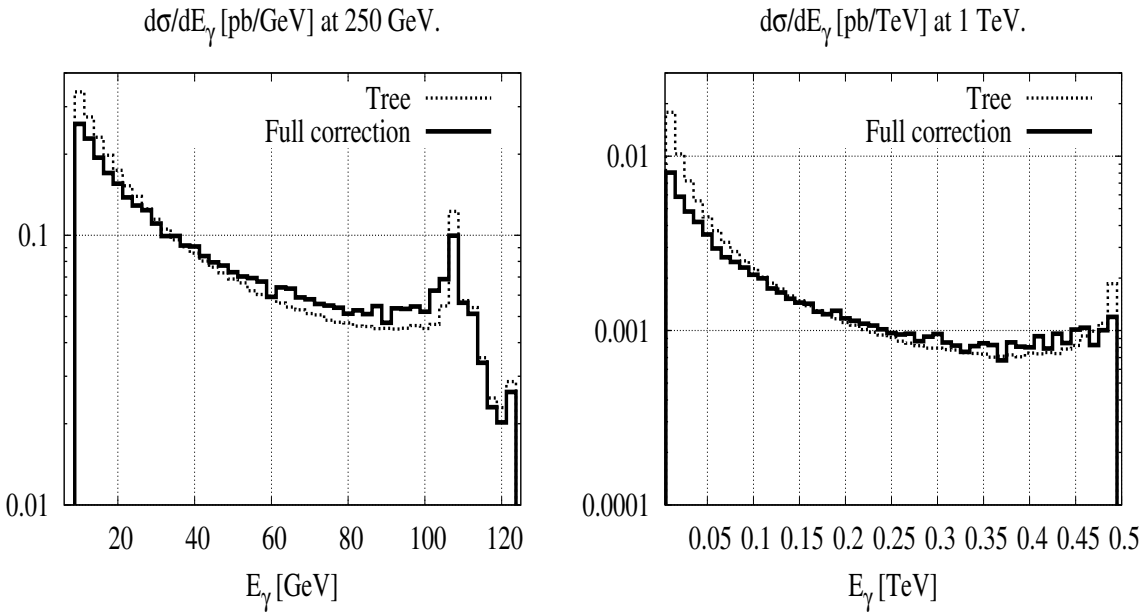


Figure 3: The differential cross-section as a function of the photon energy at $\sqrt{s} = 250$ GeV and $\sqrt{s} = 1$ TeV.

# 4 Conclusions

The QED and full $\mathcal{O}(\alpha)$ electroweak radiative corrections to $e^+e^- \to e^+e^-\gamma$ at the International Linear Collider have been calculated successfully by using the GRACE-Loop system.

This system incorporates a generalised non-linear gauge fixing condition which includes five gauge parameters. Together with the UV, IR finiteness this provides a powerful tool to test the consistency of the results. In the numerical checks of this calculation, we find that the results are numerically stable when quadruple precision is used.

In the physics results of the full electroweak corrections we find that the numerical value of the full electroweak radiative corrections vary from $-2\%$ to $\sim -20\%$ in the range

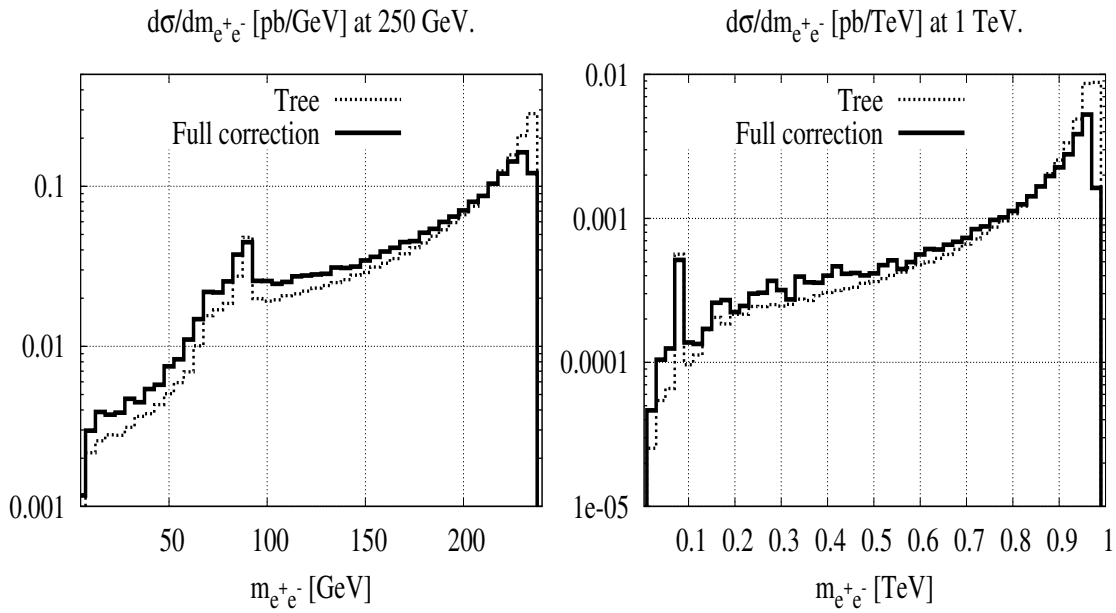


Figure 4: The differential cross-section as a function of the invariant mass of the $e^-$, $e^+$ pair. At the left $\sqrt{s} = 250$ GeV and at the right $\sqrt{s} = 1$ TeV.

of 250 GeV to 1TeV for the center-of-mass energy. Therefore this calculation is important for the determination of the luminosity at the ILC.

# Acknowledgments

We wish to thank Prof. F. Yuasa and Dr. N. Watanabe for valuable discussions and comments. The authors are grateful to Prof. K. Tobimatsu and Prof. M. Igarashi for useful discussions and their contributions. The work of T.U. was supported by the DFG through SFB/TR 9 "Computational Particle Physics".

# References


[1] K.Tobimatsu and Y.Shimizu, Prog. Theor. Phys. **74** (1985), 567-575.

[2] K.Tobimatsu and Y.Shimizu, Prog. Theor. Phys. **75** (1986), 905-913.

[3] M. Bohm, A. Denner, W. Hollik and R. Sommer, Phys. Lett. B **144** (1984) 414.

[4] M. Bohm, A. Denner and W. Hollik, Nucl. Phys. B **304** (1988) 687.

[5] F. A. Berends, R. Kleiss and W. Hollik, Nucl. Phys. B **304** (1988) 712.

[6] J. Fleischer, J. Gluza, A. Lorca and T. Riemann, Eur. J. Phys. **48** (2006) 35 [hep-ph/0606210].

[7] A. A. Penin, Phys. Rev. Lett. **95** (2005) 010408 [hep-ph/0501120].

[8] A. A. Penin, Nucl. Phys. B **734** (2006) 185 [hep-ph/0508127].

[9] R. Bonciani, A. Ferroglia, P. Mastrolia, E. Remiddi and J. J. van der Bij, Nucl. Phys. B **701** (2004) 121 [hep-ph/0405275].

[10] R. Bonciani, A. Ferroglia, P. Mastrolia, E. Remiddi and J. J. van der Bij, Nucl. Phys. B **716** (2005) 280 [hep-ph/0411321].

[11] R. Bonciani, A. Ferroglia and A. A. Penin, Phys. Rev. Lett. **100** (2008) 131601 [arXiv:0710.4775 [hep-ph]].

[12] R. Bonciani, A. Ferroglia and A. A. Penin, JHEP **0802** (2008) 080 [arXiv:0802.2215 [hep-ph]].

[13] S. Actis, P. Mastrolia and G. Ossola, Phys. Lett. B **682** (2010) 419 [arXiv:0909.1750 [hep-ph]].

[14] A. A. Penin and G. Ryan, JHEP **1111** (2011) 081 [arXiv:1112.2171 [hep-ph]].

[15] K. Tobimatsu and M. Igarashi, Comput. Phys. Commun. **136** (2001) 105.

[16] M. Igarashi et al, *in preparation.*

[17] G. Belanger, F. Boudjema, J. Fujimoto, T. Ishikawa, T. Kaneko, K. Kato and Y. Shimizu, Phys. Rept. **430**, 117 (2006) [hep-ph/0308080].

[18] G. Belanger, F. Boudjema, J. Fujimoto, T. Ishikawa, T. Kaneko, Y. Kurihara, K. Kato and Y. Shimizu, Phys. Lett. B **576** (2003) 152 [hep-ph/0309010].

[19] G. Belanger, F. Boudjema, J. Fujimoto, T. Ishikawa, T. Kaneko, K. Kato, Y. Shimizu and Y. Yasui, Phys. Lett. B **571**, 163 (2003) [hep-ph/0307029].

[20] G. Belanger, F. Boudjema, J. Fujimoto, T. Ishikawa, T. Kaneko, K. Kato and Y. Shimizu, Nucl. Phys. Proc. Suppl. **116**, 353 (2003) [hep-ph/0211268].

[21] R. -Y. Zhang, W. -G. Ma, H. Chen, Y. -B. Sun and H. -S. Hou, Phys. Lett. B **578** (2004) 349 [hep-ph/0308203].

[22] Y. You, W. -G. Ma, H. Chen, R. -Y. Zhang, S. Yan-Bin and H. -S. Hou, Phys. Lett. B **571** (2003) 85 [hep-ph/0306036].

[23] A. Denner, S. Dittmaier, M. Roth and M. M. Weber, Phys. Lett. B **575** (2003) 290 [hep-ph/0307193].

[24] A. Denner, S. Dittmaier, M. Roth and M. M. Weber, Nucl. Phys. B **680** (2004) 85 [hep-ph/0309274].

[25] A. Denner, S. Dittmaier, M. Roth and M. M. Weber, Phys. Lett. B **560** (2003) 196 [hep-ph/0301189].

[26] A. Denner, S. Dittmaier, M. Roth and M. M. Weber, Nucl. Phys. B **660** (2003) 289 [hep-ph/0302198].

[27] K. Kato, F. Boudjema, J. Fujimoto, T. Ishikawa, T. Kaneko, Y. Kurihara, Y. Shimizu and Y. Yasui, PoS HEP **2005** (2006) 312.

[28] K. Aoki, Z. Hioki, R. Kawabe, M. Konuma and T. Muta, Suppl. Prog. Theor. Phys. **73** (1982) 1.

[29] G. J. van Oldenborgh, *Comput. Phys. Commun.* **58** (1991) 1.

[30] T. Hahn, `LoopTools`, `http://www.feynarts.de/looptools/`.

[31] F. Boudjema and E. Chopin, *Z. Phys.* **C73** (1996) 85; hep-ph/9507396.

[32] P. H. Khiem, J. Fujimoto, T. Ishikawa, T. Kaneko, K. Kato, Y. Kurihara, Y. Shimizu and T. Ueda *et al.*, Eur. Phys. J. C **73** (2013) 2400 [arXiv:1211.1112 [hep-ph]].

[33] S. Kawabata, *Comp. Phys. Commun.* **41** (1986) 127; *ibid.,* **88** (1995) 309.

[34] http://www.mcs.anl.gov/research/projects/mpi/

[35] T. Ishikawa, T. Kaneko, K. Kato, S. Kawabata, Y. Shimizu and H. Tanaka, KEK Report 92-19, 1993, `GRACE` manual Ver. 1.0.

[36] A. Denner and S. Dittmaier, Nucl. Phys. B **734** (2006) 62 [hep-ph/0509141].